Differential n-p Scattering Cross Section for 220-Mev Neutrons*

G. GUERNSEY,† G. MOTT,‡ AND B. K. NELSON§
Department of Physics, University of Rochester, Rochester, New York
(Received March 10, 1952)

The differential neutron-proton scattering cross section as a function of angle has been investigated for neutron energies of 220 Mev and 180 Mev. A ½-inch Be target at the 58¼-inch radius in the University of Rochester 130-in. cyclotron was used to produce a beam of neutrons. This neutron beam scattered protons from a polyethylene scatterer which were detected by a four scintillation counter coincidence telescope. A measurement of the pulse height from the last counter was used to determine the energy of the scattered proton. The effect of the carbon in the polyethylene was subtracted by taking runs with a carbon scatterer calculated to have the same number of carbon atoms per cm² as had the polyethylene. Runs were taken from 0° to 50° for the proton angle in the laboratory coordinate system. A comparison is made of the 220-Mev angular distribution with the Berkeley 260-Mev data which indicates essential agreement of the shapes.

INTRODUCTION

THE characteristic of the neutron-proton scattering problem which has become increasingly difficult to cope with, as experiments have advanced to higher energies, is that of specifying the energy of the neutron which is being scattered. It is, of course, desirable to do this with as high a counting efficiency as possible, and still determine the energy accurately. The problem has been solved in this experiment by detecting protons with a scintillation counter telescope, the last counter of which was calibrated for its pulse-height response to proton energy. Since only thin crystal anthracene counters need be used in the quadruple coincidence telescope, the protons lost to the detector are negligible. Also, since the shape of the resolution curve for monoenergetic protons can be determined for the last counter as well as its pulse-height response *versus* proton energy, the proton energy determination can be made to a few percent.

This experiment is one of a group of three high energy neutron studies and the methods and apparatus used are in general the same as those described in the first two[1,2] and in a subsequent paper.[3] The methods will be described only where they differ from those of reference 1. The notations for angles and the kinematic relations of the neutron and proton are those given in the paper by Hadley *et al.*[4] The definition of angles is repeated here for convenience: Φ is the angle that the proton makes in the laboratory system with the direction of the incident neutron and θ is the center-of-mass angle of the scattered neutron.

The geometry of the counter telescope employed is presented in Fig. 1. It is the scatterer S and counter C_3 that determine the maximum spread $\delta\Phi$ in the angle Φ, and the distance from S to C_3 as well as the area of C_3 that determine the solid angle $\Delta\omega$ for any point in the scatterer. The angular resolution curve is essentially triangular in the approximation that $\tan\delta\Phi=\delta\Phi$ and that the widths of S and C_3 are equal. For the geometry shown, $\delta_{\max}\Phi=5°$ full width at the base of the triangle and $\Delta\omega=1.8\times10^{-3}$ steradian. For the short telescope run (Group B), to be mentioned later, $\Delta\omega=5.85\times10^{-3}$ steradian.

The pulse-height spectra for protons scattered into the counter telescope have been recorded for telescope angles of from 0° to 50° as measured from the incident neutron direction. From this the number of protons per unit pulse height, at pulse heights corresponding to a constant neutron energy, has been determined for each angle. This number of protons is then transformed to a proton energy scale and finally to a neutron energy scale from the kinematics of the scattering. The number of protons per Mev of the incident neutron energy is proportional to the laboratory system cross section and can be converted to the center-of-mass system by multiplying by the appropriate value of $d(\cos\Phi)/d(\cos\theta)$. If we call this $R(\theta)$, then $R(\theta)$ is related to the absolute value of the cross section $\sigma(\theta)$ by requiring that

$$\int KR(\theta)d\omega=\sigma_{\text{tot}}, \quad \text{for} \quad \sigma(\theta)=KR(\theta). \qquad (1)$$

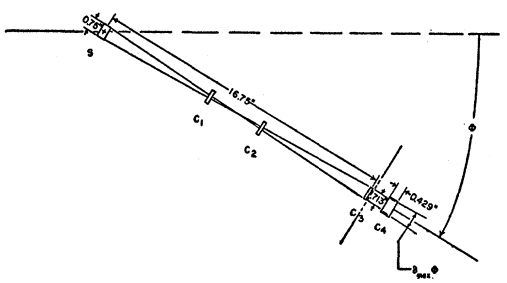

FIG. 1. Counter geometry.

* This work was assisted by the research program of the AEC.
† Now at Massachusetts Institute of Technology (Project Lincoln), Cambridge, Massachusetts.
‡ Now at Medical Center, University of Rochester, Rochester, New York.
§ Now at Massachusetts Institute of Technology (Project Lincoln), Cambridge, Massachusetts.
[1] Nelson, Mott, and Guernsey, accompanying paper [Phys. Rev. 88, 1 (1952)].
[2] Mott, Guernsey, and Nelson, preceding paper [Phys. Rev. 88, 9 (1952)].
[3] Guernsey, Mott, Nelson, and Roberts, Rev. Sci. Instr. 23, 476 (1952).
[4] Hadley, Kelly, Leith, Segrè, Wiegand, and York, Phys. Rev. 75, 351 (1949).

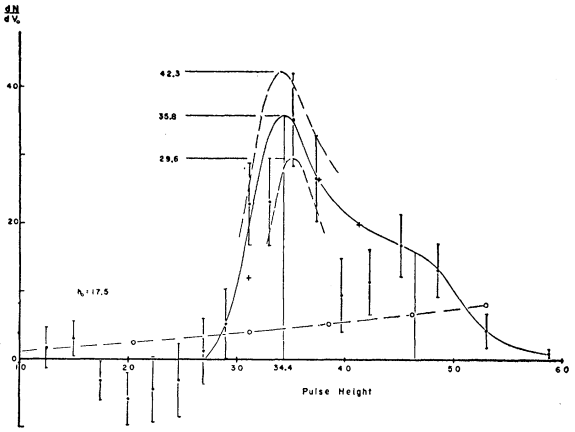

FIG. 2. Pulse-height distribution for $\Phi=50°$, recoil protons, showing the low energy contribution. The small solid circles represent the observed number of protons per unit pulse height with their statistical uncertainties. The large circles correspond to contributions from neutron energies below 166 Mev, the crosses to contributions from neutron energies above 166 Mev, both of which have been computed from a measured neutron spectrum.

NEUTRON SPECTRUM

The energy spectrum of the incident neutrons is that of Fig. 4(b) in reference 1, and is described in detail in reference 1. (See also Fig. 3 of this paper.)

ANALYSIS OF THE DATA

The method of analysis applied to the data is essentially that of steps (a) through (e) in reference 1 with the exception that here we were concerned with obtaining dN_p/dE_n for a particular value of E_n rather than for the entire spectrum. The value of E_n considered was 220 Mev since this corresponded to the peak of the neutron spectrum (and thus the peaks of the pulse-height distributions) where the counting statistics were of course the best. Data for $E_n=180$ Mev were also considered and are presented here only as an illustration of the further possibilities of this method. For the neutron spectrum used, the counting rates in the pulse-height spectra were appreciably lower at 180 Mev, and thus the statistics are quite poor.

The energy determination was made by averaging the neutron energies corresponding to the pulse heights at the peaks of eighteen pulse-height spectra. This gives an average deviation from the average of 2.2 percent and is an indication of the relative accuracy of the determination. However, the absolute value is in doubt through some, as yet, unknown error and is believed to be 215 Mev for the peak of the spectrum used here. One is referred to the Run Calibration section of reference 1 for comment on this discrepancy.

In Fig. 2 is an example of the data recorded in the form of a pulse-height distribution for $\Phi=50°$. This particular distribution has rather poor statistical accuracy. However, it is a good example of an important characteristic of this method of detection. The number of protons per unit pulse height at the peak, $dN_p/dV_0 = 35.8\pm6.2$, is the number to be transformed to a value of dN_p/dE_n which is proportional to $\sigma(\Phi=50°)$. The observed position of the peak is 34.4 volts (on an arbitrary scale) and the 17.5 is from the associated calibrating proton run, indicating that 193-Mev protons appear at 17.5 volts rather than the standard 16.95 and the pulse-height scale must undergo a corresponding linear transformation.

DOUBLE-VALUED PULSE-HEIGHT SPECTRUM

Consider the energy of the proton scattered by a neutron of energy E_n. The proton will lose energy as it passes through the remainder of the scatterer, the three coincidence crystals and into the last (proportional) counter crystal. Thus for some value of E_n, at a given angle Φ, the protons will stop at the far face of the last counter, losing the maximum energy in the crystal and thus giving the maximum pulse height. Protons, from neutrons above this energy (E_{nc}) as well as from neutrons below E_{nc}, will lose less energy and so give smaller pulse heights. Therefore, it is evident that the pulse-height distribution is double valued. For small angles Φ, and the counter 4 crystal thickness used (1.09 cm), E_{nc} is quite small. Since the low energy end of the neutron spectrum is sparsely populated, this means that the contribution to the pulse-height spectrum from the low energy end of the neutron spectrum is also quite small. However, for large laboratory angles, E_{nc} includes an appreciable portion of the neutron spectrum (at $\Phi=50°$, $E_{nc}=166$ Mev) and the low energy contribution is no longer negligible. In Fig. 2 the protons scattered by neutrons of energy below 166 Mev are shown by the dashed line.

The neutron spectrum referred to above is shown in Fig. 3. The measured values extend to 142 Mev and

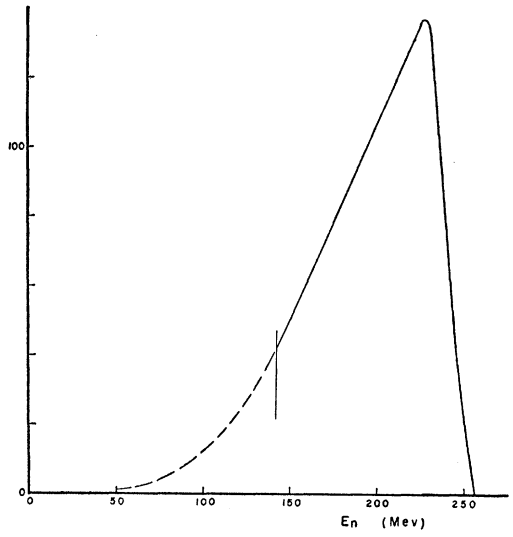

FIG. 3. The differential neutron spectrum, at 0° from ½-in. Be target, assumed as effective in the scattering experiment including the extrapolation used for the low energy corrections. The solid line is an observed spectrum (reference 1).

have been extrapolated as shown by the dashed line. This spectrum was transformed by the inverse of the steps described in reference 1 into a proton pulse-height distribution for the value of Φ in question. For this correction, it was assumed that the cross section is proportional to $1/E$. Also, it was necessary to assume something about the response of counter 4 to protons of energy below about 45 Mev, the low energy end of our calibration.

The largest pulses observed correspond to protons of energy 37.5 Mev which have a range of 1.09 cm of anthracene. (See appendix of reference 3.) The calibration curve was, therefore, extrapolated to a pulse height of 51.3 volts for 37.5 Mev, as obtained from a $\Phi=50°$ recoil proton spectrum from a carbon scatterer. This had a reasonably sharp cutoff at 51.3 units of pulse height. The remainder of the pulse height *versus* energy curve was assumed to follow a straight line, pulse height in volts $=1.368$ times the proton energy in Mev, from 0 to 37.5 Mev.

The points indicated by large circles in Fig. 2 correspond to neutron energies below $E_{nc}(50°)=166$ Mev and the three crosses refer to points above 166 Mev. The low energy points were normalized by requiring that the three high energy points, with the low energy contribution added, should fit the observed pulse-height spectrum. The correct number per unit pulse height is obtained by subtracting the low energy contribution from the observed value, as $35.8\pm6.2-4.5=31.3\pm6.2$ counts per unit pulse height. This correction amounts to about 12 percent for $\Phi=50°$, $E_n=220$ Mev, 40 percent at the same angle for $E_n=180$ Mev. Since, this correction is less than 1.5 percent for $\Phi=40°$, $E_n=220$ Mev and 4 percent for $\Phi=40°$, $E_n=180$ Mev, it was not made for angles less than $\Phi=40°$.

EXPERIMENTAL RESULTS

All values of $\sigma(\theta)$ obtained from $E_n=220$ Mev are presented in Table I. Group B data were run with a wider acceptance angle telescope and has been normalized to a smooth curve through the five points of Group A. The average deviation of the Group B data from the normalizing ratio was 2.0 percent. The two

TABLE I. $\sigma(\theta)$ in 10^{-27} cm^2/sterad for $E_n=215$ Mev. $\sigma(\theta)=KR(\theta)$, $K=0.0468$.

Φ	$\frac{d\cos\Phi}{d\cos\theta}$	$\sigma(\theta)$[a] $A_\circ$	$B^\square$	C^x	$D^\triangle$	Weighted average	θ
0	0.2238				13.4 ±2.8	13.4 ±2.8	180
7.5	0.2266	8.89±0.84		8.84±1.03		8.89±0.66	164.2
10	0.2288				7.58±0.75	7.58±0.75	158.8
10.7	0.2296		6.97±1.31			6.97±1.31	157.3
15	0.2353	5.43±0.66		4.77±0.89		5.38±0.47	148.4
				5.90±1.03			
19.1	0.2427		4.23±0.48			4.18±0.35	139.9
			4.13±0.52				
29.8	0.2730		2.53±0.37			2.53±0.37	117.7
30	0.2737	2.47±0.42		2.29±0.51		2.40±0.32	117.2
40	0.3211	1.29±0.20	1.41±0.20	1.19±0.25		1.31±0.12	96.9
50	0.3976	1.43±0.28	1.47±0.39			1.45±0.22	76.9

[a] Columns A through D are results of four different runs [see text]. The symbols refer to Fig. 4.

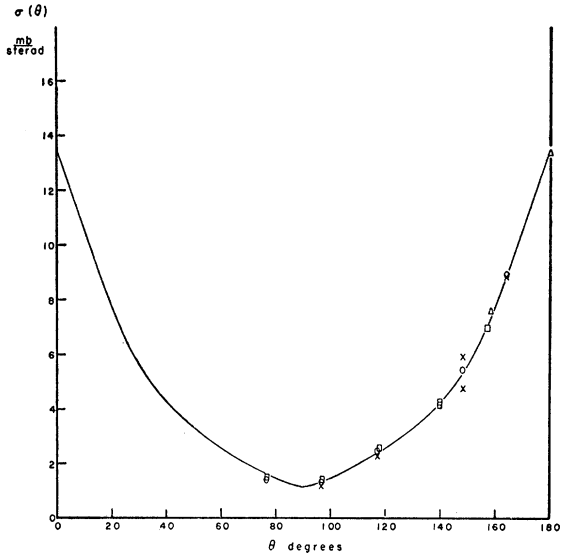

FIG. 4. All experimental determinations of differential cross section for 220-Mev neutron energy. The symbols refer to Table I. The smooth curve is an empirical fit used only for normalization to the total cross section.

points of Group D were also normalized to Group A using the 10° point of Group D (the only point in the range common to both, which was 5.5 percent higher than the smooth curve for Group A. Group C is presented just as obtained per 1000 monitor counts with no renormalization.

The errors given are the result of counting statistics alone. They correspond very closely to the standard deviations on the individual points in the original polyethylene-carbon differences, but in most cases are derived from two extreme curves drawn for the pulse-height distributions. (See the upper and lower partial curves in Fig. 2.)

The variation of the cross section over the angular width of the telescope is negligible except for the point at $\Phi=0°$. At 0°, however, the cross section falls off rapidly over the entire 2π of directions from 0° and, as a result, the value of $(dN_p/dE_n)(\Phi=0°)$ would give a too low value of $\sigma(180°)$. This effect has been calculated using the triangular window for Φ mentioned above and a straight line for $(dN_p/dE_n)(\Phi)$ required to contain the $\Phi=7.5°$ point. The correction amounts to an increase of 4.4 percent and has been applied to the value of $\sigma(\theta=180°)$ given in Table I.

NORMALIZATION TO THE TOTAL CROSS SECTION

Since the experimental points do not extend very far below $\theta=90°$, it is difficult to make an extrapolation of the points to $\theta=0°$. Therefore, a smooth curve was drawn through the weighted averages of the points from 180° to 90° and Eq. (1) was rewritten as

$$\sigma_{\text{tot}}\simeq 2\pi K\cdot\frac{2\pi}{18}\sum_{n=0}^{8}R(95+10n)\sin(95+10n).$$

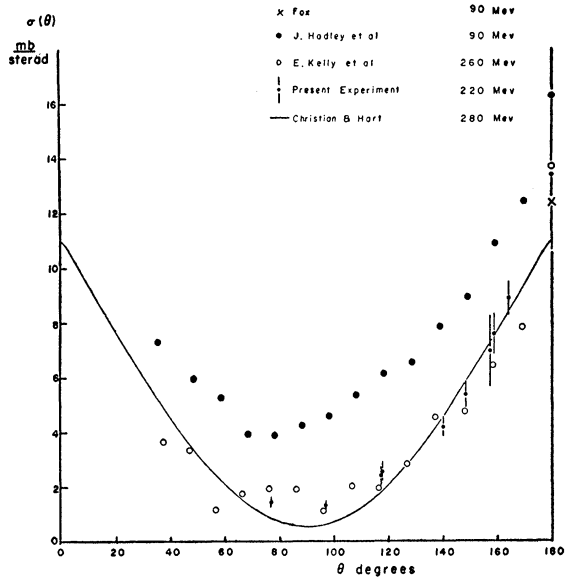

FIG. 5. The weighted averages of the 220-Mev data, plotted for comparison of the shapes with the Berkeley data and the theoretical prediction of Christian and Hart for a tensor force model. The absolute values are not directly comparable, since the 220-Mev data have been normalized for 90° symmetry and the 260-Mev data for $\theta<90°$ symmetry.

For the curve shown in Fig. 4, $K=0.0468$, when the total n-p cross section is taken equal to $41.3\pm3.5\times10^{-27}$ cm^2. This is the value given in reference 2 for $E_n=220$ Mev. Figure 4 also presents all the values of $\sigma(\theta)$ given in Table I.

If the data had been normalized to the same shape curve but symmetric about 85° instead of symmetric about 90°, the absolute values of the points would then be 13 percent higher. The ±8.5 percent assigned to the total cross section also contributes to the error in the absolute values of $\sigma(\theta)$.

Unfortunately, one can say nothing much from the data regarding symmetry about 90°. However, from whatever minimum is evident in going as far as $\theta=77°$, the data are in essential agreement with the finding by Christian and Hart[5] of slightly greater than 50 percent

TABLE II. $\sigma(\theta)$, 10^{-27} cm^2/sterad. $E_n=172$ Mev $K=0.144$.

Φ	$\frac{d\cos\Phi}{d\cos\theta}$	$\sigma(\theta)$[a] A°	$B\square$	C^z	D^Δ	Weighted average	θ
0	0.2282				16.6±6.8	16.6±6.8	180
7.5	0.2311	9.7±1.3		13.0±3.0		10.9±1.4	164.5
10	0.2330				7.6±1.5	7.6±1.5	159.3
10.7	0.2338		7.0±1.2			7.0±1.2	157.8
15	0.2392	4.8±1.0		4.9±1.3		5.3±0.8	148.8
				6.4±1.8			
19.1	0.2464		4.2±1.2			3.5±0.9	140.5
			2.5±1.1				
29.8	0.2758		2.1±0.9			2.1±0.9	118.2
30	0.2762	2.8±0.8		2.0±1.0		2.5±0.6	117.7
40	0.3219	3.0±0.6	2.1±0.6			2.4±0.4	97.4
50	0.3960	2.3±0.7				2.3±0.7	77.5

[a] Data corresponding to values in columns A through D are identified in text in connection with Table I. Symbols refer to Fig. 6.

[5] R. S. Christian and E. W. Hart, Phys. Rev. **77**, 441 (1950).

exchange force giving a good fit to the high energy angular distributions.

One may compare the weighted averages of our data for $E_n=220$-Mev, taken from Table I, with the Berkeley data for 90-Mev[4,6] and 260 Mev[7] by referring to Fig. 5. The additional 90-Mev point at 180° was obtained from Fig. 12 of reference 6 and is due to Fox.[8] The 220-Mev data overlap to some extent, but are on the average higher than that at 260 Mev. It may be noted that the ratios $\sigma(180°)/\sigma(90°)$ are about equal for the 220-Mev and 260-Mev distributions. However, since the ratios are so large at these energies, the experimental errors do not justify a precise comparison.

The solid curve in Fig. 5 is a theoretical prediction of Christian and Hart[5] for n-p scattering from a Yukawa potential at 280-Mev neutron energy, with

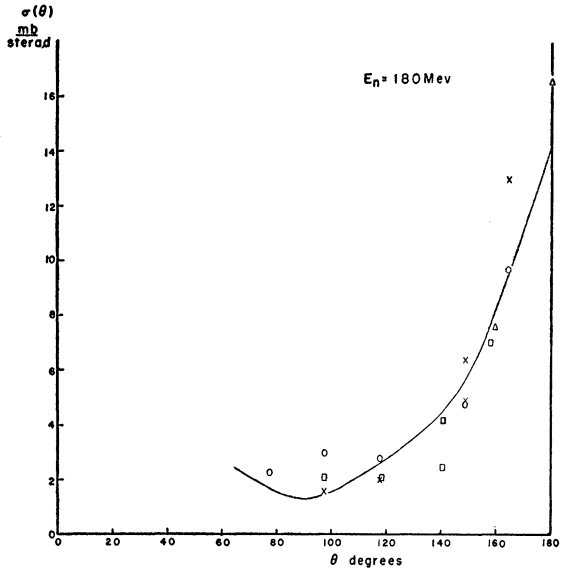

FIG. 6. Values of $\sigma(\theta)$ obtained from the pulse-height distribution data at a pulse height other than that of the maximum of the distribution. The solid curve is the same shape used for normalizing the 220-Mev data. The symbols refer to Table II.

inclusion of tensor force, for a $\sigma_{tot}=37\times10^{-27}$ cm^2 and has been copied from Fig. 3 of reference 6. One observes that, for the symmetric normalization used in the case of $\sigma(\theta, 220$ Mev), this curve is about as good a fit to the 220-Mev data as it is to the 260-Mev data of the Berkeley group. An additional comment may be made regarding the shape of the angular distribution presented here. It seems to satisfy the description of being V-shaped rather than U-shaped, thus being consistent with the inclusion of a tensor interaction in the potential model.

The values of $\sigma(\theta)$ for $E_n=180$ Mev, obtained from the pulse-height spectra which furnished the $E_n=220$-

[6] Chamberlain, Segrè, and Wiegand, Phys. Rev. **83**, 923 (1951).
[7] Kelly, Leith, Segrè, and Wiegand, Phys. Rev. **79**, 96 (1950).
[8] R. H. Fox, unpublished USAEC Report No. UCRL-867 (1950).

Mev information, are presented in Table II. They have been calculated in the same way as were the values for $E_n=220$, except that the effects of finite pulse-height resolution and angular resolution have been neglected. This is justified when the pulse-height spectra do not change slope rapidly compared with the resolution widths. These values of $\sigma(\theta)$ for 180 Mev are plotted in Fig. 6, in which the solid curve is the same as was used for integration of the 220-Mev data but normalized to a total cross section of 44 mb.[2] The value of K taken for these data was 0.144, which fitted the points to the normalizing curve more or less closely. This distribution exhibits the expected gross features, but details of shape, unfortunately, are not significant.

The authors wish to express their appreciation to Professsor A. Roberts for his interest in this problem and his generous assistance with the performance and analysis of the experiment.

PHYSICAL REVIEW VOLUME 88, NUMBER 1 OCTOBER 1, 1952

Excitation Functions to 100 Mev*

NORTON M. HINTZ† AND NORMAN F. RAMSEY
Nuclear Laboratory, Harvard University, Cambridge, Massachusetts
(Received June 2, 1952)

A method is described for obtaining excitation functions using the stacked foil technique with an internal cyclotron beam. The method, which utilizes multiple Coulomb scattering for deflection and 180° focusing for energy separation, has the advantages of good energy resolution, high intensity, and low background. Equations are presented for the particle orbits from which are derived the energy resolution and efficiency attainable. Absolute excitation curves are given for the reactions, $C^{12}(p,pn)C^{11}$; Na^{24}, Na^{22}, and F^{18} from Al^{27}; $B^{11}(p,n)C^{11}$; and $S^{34}(p,n)Cl^{34}$. Absolute cross sections are determined using the monitor reaction, $C^{12}(p,pn)C^{11}$, and the ratio of the β-counting rates. Various corrections to the relative and absolute excitation curves are discussed. A brief interpretation of the results is given in which it is argued that they are consistent with present ideas about high energy nuclear reactions.

1. INTRODUCTION

THE sparsity of data on excitation functions of nuclear reactions above 30 Mev made it worthwhile to begin a systematic study in this field with the 100-Mev protons from the Harvard cyclotron. Some of the results of this investigation have already been published[1–3] together with a brief account of the method used. It is the purpose of this paper to describe the method more fully and to present some additional excitation curves.

At energies of a few tens of Mev one expects individual variations in nuclear structure to have little effect on the excitation curves, the main features of which should depend on the more general properties of nuclei such as the average nucleon density, the momentum distribution of the nucleons, the mean free path of fast nucleons in nuclear matter, and the average level density at large excitation. Accordingly, it was felt that a method should be devised by means of which a few reactions could be done with reasonably high accuracy, especially those which were of particular use in monitoring high energy proton flux, and by means of which the main features of a large number of other reactions could be obtained quickly and with economy of cyclotron time.

The classical method of stacked foils[4] satisfies these requirements well at low energies where no special difficulties are met with in beam deflection, extraction, and intensity. However, at 100 Mev, the present techniques of extraction are highly inefficient and therefore lead to serious problems of intensity or energy resolution. To overcome these difficulties it was decided to use the stacked foil method with the internal cyclotron beam, making use of the focusing properties of the uniform magnetic field to provide a nearly monochromatic beam of reasonable intensity. A somewhat similar technique has been used by Chupp and McMillan[5] with the protons stripped from fast deuterons. However, due to the broad energy distribution of their protons, the choice of carbon as an absorber, and the high neutron background their results were inaccurate.

2. EXPERIMENTAL GEOMETRY AND PARTICLE ORBITS

The method of stacked foils is unsatisfactory for use directly with the circulating beam of a frequency modulated cyclotron for two reasons. First, the small gain in orbit radius per turn (~1 mil) makes it impossible to align the foil and absorber assembly in such a way that all targets receive the same proton flux.

* Assisted by the joint program of the ONR and AEC.
† Present address: Department of Physics, University of Minnesota, Minneapolis, Minnesota.
[1] Norton M. Hintz, Phys. Rev. **83**, 185 (1951).
[2] J. W. Meadows and R. B. Holt, Phys. Rev. **83**, 47 (1951).
[3] J. W. Meadows and R. B. Holt, Phys. Rev. **83**, 1257 (1951).
[4] E. O. Lawrence, Phys. Rev. **47**, 17 (1935).
[5] W. W. Chupp and E. M. McMillan, Phys. Rev. **72**, 873 (1947).